Partial Pole Placement using Static Output Feedback

Manuel Pusch * **Julian Theis** ** **Daniel Ossmann** ***

* *Institute of System Dynamics and Control, German Aerospace Center (DLR), 82234 Weßling, Germany (e-mail: manuel.pusch@dlr.de)*
** *Institute of Aircraft Systems Engineering, Hamburg University of Technology, 21129 Hamburg, Germany (e-mail: julian.theis@tuhh.de)*
*** *Dept. of Mechanical, Automotive and Aeronautical Engineering, Munich University of Applied Sciences, 80335 Munich, Germany (e-mail: daniel.ossmann@hm.edu)*

Abstract: For many dynamical systems it is required to specifically shift individual poles, especially when these poles are lightly damped or even unstable. To achieve that, a preferably large number of effectors and measurements are installed leading to multivariable control problems. In this paper, a novel control approach is presented for placing either a single pole or a conjugate complex pole pair at a predefined location using rank-one static output feedback. Rank-one feedback can be interpreted as blending inputs and outputs to define a single input and single output loop with a desirable root locus along which the pole is moved. The corresponding controller synthesis is reduced to an unconstrained optimization problem in a single variable that aims at minimizing the feedback gain. Although the approach is derived for a single pole or conjugate complex pole pair, it is easily extended to multiple poles. To this end, a repeated design and superposition of rank-one feedback gains is proposed. It is further shown how residual system dynamics as well as subsequently designed gains can be efficiently decoupled from each other in order to avoid undesired interactions and spillover effects. The effectiveness of the proposed control approach is demonstrated by means of a numerical example.

Keywords: static feedback control, multivariable systems, pole assignment, blending of inputs and outputs, modal control

1. INTRODUCTION

Most design approaches in control engineering explicitly (e.g., root locus method or pole placement) or implicitly (e.g., time domain optimization) place the system's poles at desired locations in the complex left half-plane. When all states of the system are measured, pole placement can be achieved via full state feedback. If this is not possible, state estimation methods can be applied, which introduce dynamics into the control system. Alternatively, static output feedback can be used for pole placement when a sufficient number of adequate control inputs and measurement outputs are available. Various necessary and sufficient conditions for arbitrary pole placement via static output feedback have been formulated. Obviously, all states of the dynamic system must be both controllable and observable. Wang (1992) showed that it is then sufficient for a generic system with n_u inputs, n_y outputs, and n_x states that $n_u n_y > n_x$. Other conditions are derived, e.g., by Willems and Hesselink (1978); Kimura (1994); Kiritsis (2002) and serve as a basis for developing different controller synthesis algorithms. An overview of the vast amount of synthesis methods is given, e.g., by Rosenthal and Willems (1999); Syrmos et al. (1997) or in more recent publications by Yang and Orsi (2007); Franke (2014).

In general, the optimization problem for arbitrary pole placement using static output feedback is non-convex and its complexity increases with the number of inputs and outputs. To tackle this issue, control methods have been developed which facilitate controller design by decoupling and placing each pole of interest individually. This is of special concern for many practical applications in which only a few dominant poles out of a large number of poles need to be shifted. Related control approaches are described by Danowsky et al. (2013); Hoogendijk et al. (2014); Pusch (2018) and have been successfully validated in Danowsky et al. (2018); Pusch et al. (2019). Therein, the basic idea is to control an individual dynamic mode, described by a conjugate complex pair of eigenvalues and -vectors of the system matrix, by means of a single-input and single-output (SISO) controller. To that end, the n_u control inputs and n_y measurement outputs are blended by real-valued vectors such that, ideally, a SISO system representing the target mode is obtained. The advantage is that multivariable controller design is split up into two separate but more intuitive and easier tunable parts: a blending vector design and a subsequent SISO controller design, which are repeated for each mode to be controlled.

In this paper, a novel control approach is presented which selects the blending vectors so that the target mode is isolated and constant feedback shifts its pole pair as desired. In this way, a static output feedback controller of rank one is obtained. It consists of the two blending vectors scaled by the scalar feedback gain. The proposed approach generalizes the method of Pusch and Ossmann (2019a), where the same type of controller is used to increase relative damping of a conjugate complex pole pair. A numerically efficient algorithm for computing the controller is derived in Section 3, based on the modal decomposition described in Section 2. Eventually, the applicability of the approach is demonstrated by means of a numerical example in Section 4.

2. MODAL DECOMPOSITION OF LTI SYSTEMS

A linear time-invariant (LTI) system with n_u inputs, n_y outputs and n_x states which is physically realizable can be represented in state space as

$$G: \quad \begin{bmatrix} \dot{x} \\ y \end{bmatrix} = \left[\begin{array}{c|c} A & B \\ \hline C & D \end{array}\right] \begin{bmatrix} x \\ u \end{bmatrix}, \tag{1}$$

where $A \in \mathbb{R}^{n_x \times n_x}$, $B \in \mathbb{R}^{n_x \times n_u}$, $C \in \mathbb{R}^{n_y \times n_x}$, $D \in \mathbb{R}^{n_y \times n_u}$. In case $D = 0$, the LTI system G is called *strictly proper*. Assuming that A is diagonalizable, the real Jordan normal form (Kailath, 1980) of G can be computed as

$$G_{\mathrm{JNF}}: \quad \begin{bmatrix} \dot{\xi}_1 \\ \vdots \\ \dot{\xi}_{n_i} \\ \hline y \end{bmatrix} = \left[\begin{array}{ccc|c} A_1 & & 0 & B_1 \\ & \ddots & & \vdots \\ 0 & & A_{n_i} & B_{n_i} \\ \hline C_1 & \dots & C_{n_i} & D \end{array}\right] \begin{bmatrix} \xi_1 \\ \vdots \\ \xi_{n_i} \\ \hline u \end{bmatrix} \tag{2}$$

by applying the similarity transformation

$$x = T\xi = [T_1 \ \dots \ T_{n_i}] \left[\xi_1^T \ \dots \ \xi_{n_i}^T\right]^T. \tag{3}$$

According to (3), the transformation matrix T consists of the sub matrices $T_i, i = 1, .., n_i$ obtained from an eigendecomposition of A. For a real eigenvalue p_i with a real eigenvector v_i, the submatrix is $T_i = v_i$ and $A_i = p_i$, $B_i = b_{p_i}$, $C_i = c_{p_i}$. For a conjugate complex pole pair $p_i = \Re(p_i) \pm \Im(p_i)$ with the conjugate complex eigenvector pair $v_i = \Re(v_i) \pm \Im(v_i)$, the submatrix is $T_i = [\Re(v_i) \ \Im(v_i)]$ and

$$\begin{aligned} A_i &= \begin{bmatrix} \Re(p_i) & \Im(p_i) \\ -\Im(p_i) & \Re(p_i) \end{bmatrix}, \ B_i = \begin{bmatrix} \Re(b_{p_i})^T \\ -\Im(b_{p_i})^T \end{bmatrix}, \\ C_i &= [\Re(c_{p_i}) \ \Im(c_{p_i})]. \end{aligned} \tag{4}$$

The vectors $b_{p_i} \in \mathbb{C}^{n_u}$ and $c_{p_i} \in \mathbb{C}^{n_y}$ are denoted the pole input and pole output vectors. Based on the real Jordan normal form (2), the output

$$y = \sum_{i=1}^{n_i} y_i + Du$$

is a superposition of the direct feedthrough Du and the responses of the individual modes

$$M_i: \quad \begin{bmatrix} \dot{\xi}_i \\ y_i \end{bmatrix} = \left[\begin{array}{c|c} A_i & B_i \\ \hline C_i & 0 \end{array}\right] \begin{bmatrix} \xi_i \\ u \end{bmatrix}. \tag{5}$$

This means that a mode M_i is a strictly proper LTI system of first (real pole) or second (conjugate complex pole pair) order and has n_u inputs and n_y outputs. Note that modes with a conjugate complex pole pair are also referred to as oscillating modes since they describe a harmonic oscillator.

Alternatively, an LTI system may also be described by a transfer function matrix, which can be derived from its state space representation (1) as

$$G(s) = C\left(sI - A\right)^{-1} B + D, \tag{6}$$

where s denotes the Laplace variable. Considering the individual mode M_i from (5), their transfer function matrices are

$$\begin{aligned} M_i(s) &= C_i(sI - A_i)^{-1}B_i \\ &= \begin{cases} \dfrac{R_1}{s - p_i} & \text{if } \Im(p_i) = 0 \\ \dfrac{R_1 s + R_0}{(s - p_i)(s - \bar{p}_i)} & \text{otherwise.} \end{cases} \end{aligned} \tag{7}$$

The residues $R_0 = \det(A_i)\, C_i A_i^{-1} B_i$ and $R_1 = C_i B_i$ are independent of the state space representation of M_i. Further, the natural frequency of a mode is $\omega_{\mathrm{n},i} = |p_i|$ and the corresponding relative damping is $\zeta_i = -\Re(p_i)/\omega_{\mathrm{n},i}$ when $\omega_{\mathrm{n},i} \neq 0$.

3. SHIFTING INDIVIDUAL POLES BY RANK-ONE STATIC OUTPUT FEEDBACK

The task of shifting the pole(s) of an individual mode $M(s) \in \{M_i(s)\}_{i=1}^{n_i}$ to a predefined location can quickly become challenging when the number of control inputs or measurement outputs is increased. To reduce the complexity of the control problem, it is proposed to use a rank-one static output feedback controller

$$K = k_u \, \lambda \, k_y^T, \tag{8}$$

where the input blending vector $k_u \in \mathbb{R}^{n_u}$ and the output blending vector $k_y \in \mathbb{R}^{n_y}$ have unit length and the gain $\lambda \in \mathbb{R}$ is minimized. The resulting control loop is given in Fig. 1, where the feedback controller K is composed as given in (8). In order to control multiple modes $M_j(s) \in \{M_i(s)\}_{i=1}^{n_i}$ with $j = 1, .., n_j$, it is proposed to design a separate rank-one controller $K_j \in \mathbb{R}^{n_u \times n_y}$ for each targeted mode and superimpose them as $K = \sum_{j=1}^{n_j} K_j$. This requires a sufficient number of inputs and outputs in order to avoid undesired interactions and spillover effects, see, e.g., the pole placement condition $n_u n_y > n_x$ discussed in Section 1.

In the following subsections, the corresponding control problem is described and efficiently solved by reformulating it as an unconstrained optimization problem in a single variable. To that end, first a controller is designed for a targeted mode without considering any residual system dynamics. Subsequently, mode decoupling constraints are added to isolate the target mode from the remaining system dynamics. Eventually, a summary of the algorithm is given to facilitate implementation.

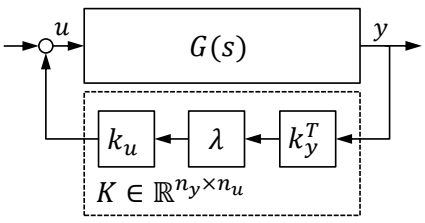

Fig. 1. Closed-loop interconnection of plant $G(s)$ with static output feedback controller K for controlling an individual mode $M(s)$.

3.1 Problem Definition

To derive the rank-one controller K from (8), its design is split into a blending vector design and a subsequent feedback gain computation. The goal is to achieve the desired closed-loop dynamics with minimum feedback gain λ and blending vectors of unit length, i.e., $|k_u| = 1$ and $|k_y| = 1$. Thus, a pair of input and output blending vectors is considered optimal for the control problem, when $|\lambda|$ is minimal.

In order to formulate the corresponding control design problem, a single oscillating mode with a conjugate complex pole pair p and $\bar{p}$ is considered. According to (7), the transfer function matrix of an oscillating mode is given as

$$M(s) = \frac{R_1 s + R_0}{(s-p)(s-\bar{p})} = \frac{R_1 s + R_0}{s^2 + 2\zeta\omega_\mathrm{n} s + \omega_\mathrm{n}^2}, \tag{9}$$

where $R_0 \in \mathbb{R}^{n_y \times n_u}$, $R_1 \in \mathbb{R}^{n_y \times n_u}$, $\omega_\mathrm{n} = |p| \neq 0$ and $\zeta = -\Re(p)/\omega_\mathrm{n}$. Blending the inputs and outputs of $M(s)$ through the vectors k_u and k_y yields

$$m(s) = k_y^T M(s)\, k_u = \frac{r_1 s + r_0}{s^2 + 2\zeta\omega_\mathrm{n} s + \omega_\mathrm{n}^2}, \tag{10}$$

with residues

$$r_0 = k_y^T R_0 k_u \quad \text{and} \quad r_1 = k_y^T R_1 k_u. \tag{11}$$

From (10), it can be seen that the blending of inputs and outputs does not change the poles of the underlying mode but rather specifies a zero at

$$z = -\frac{r_0}{r_1}. \tag{12}$$

The closed-loop transfer function for feedback of the blended outputs to the blended inputs with gain λ is obtained as

$$m_\mathrm{cl}(s) = \frac{m(s)}{1-\lambda m(s)} = \frac{r_1 s + r_0}{s^2 + \underbrace{2\zeta\omega_\mathrm{n} - \lambda r_1}_{2\zeta_\mathrm{cl}\omega_\mathrm{n,cl}} s + \underbrace{\omega_\mathrm{n}^2 - \lambda r_0}_{\omega_\mathrm{n,cl}^2}}. \tag{13}$$

In order to achieve desired closed-loop dynamics, i. e., a specified natural frequency $\omega_\mathrm{n,cl}$ and relative damping ζ_cl, the two conditions hence are

$$\omega_\mathrm{n}^2 - \lambda r_0 = \omega_\mathrm{n,cl}^2, \tag{14}$$

$$2\zeta\omega_\mathrm{n} - \lambda r_1 = 2\zeta_\mathrm{cl}\omega_\mathrm{n,cl}. \tag{15}$$

Solving (14) and (15) for r_0 and r_1, respectively, the location of the zero z from (12) is computed as

$$z = -\frac{r_0}{r_1} = -\frac{\omega_\mathrm{n}^2 - \omega_\mathrm{n,cl}^2}{2(\zeta\omega_\mathrm{n} - \zeta_\mathrm{cl}\omega_\mathrm{n,cl})}. \tag{16}$$

The case $\zeta\omega_\mathrm{n} = \zeta_\mathrm{cl}\omega_\mathrm{n,cl}$ is a singularity which is treated in Section 3.3. The singularity occurs when a conjugate complex pole pair is shifted only in the direction of the imaginary axis, i.e., $\Re(p) = \Re(p_\mathrm{cl})$. In this case, the resulting zero can be interpreted as $z = \infty$. Another special case discussed in Section 3.3 is $\omega_\mathrm{n}^2 = \omega_\mathrm{n,cl}^2$, which yields $z = 0$. In that case, the relative damping is changed without affecting the natural frequency. In other words, the conjugate complex pole pair is shifted along a circle around the origin. Both special cases are marked in Fig. 2, that illustrates the possible closed-loop locations in the complex plane for a given pole pair (✖) in dependence on the sign of z.

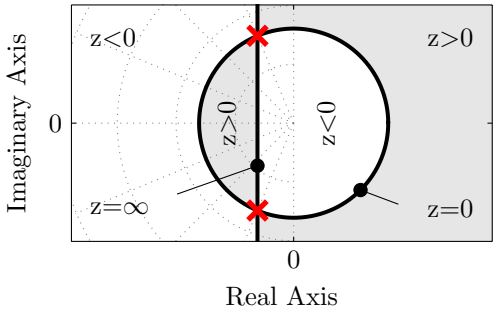

Fig. 2. Possible closed-loop pole locations for a given pole pair (✖) in the complex plane in dependence on the zero z generated by blending inputs and outputs.

In order to derive the blending vector design problem, (12) is reformulated as

$$r_0 + z r_1 = 0, \tag{17}$$

where the zero location z is specified by (16). Substituting $r_0 = k_y^T R_0\, k_u$ and $r_1 = k_y^T R_1\, k_u$ from (11) in (17), and factoring out the blending vectors k_u and k_y yields

$$k_y^T \underbrace{(R_0 + z R_1)}_{P} k_u = 0 \tag{18}$$

as a necessary constraint for k_y and k_u. To incorporate the objective of minimizing the magnitude $|\lambda|$ of the feedback gain, (15) is first reformulated as

$$\lambda = 2\,\frac{\zeta\omega_\mathrm{n} - \zeta_\mathrm{cl}\omega_\mathrm{n,cl}}{r_1}. \tag{19}$$

Doing so shows that minimizing $|\lambda|$ is equivalent to maximizing $|r_1|$. Recalling that $r_1 = k_y^T R_1 k_u$ (11) hence yields the equivalent objective function

$$\min |\lambda| \Leftrightarrow \max |k_y^T R_1 k_u|. \tag{20}$$

Combining the constraint (18) with the objective function (20), the blending vector design problem for pole placement is formulated as

$$\begin{aligned} \underset{k_u \in \mathbb{R}^{n_u}, k_y \in \mathbb{R}^{n_y}}{\text{maximize}} \quad & |k_y^T R_1 k_u| \\ \text{subject to} \quad & k_y^T P k_u = 0 \\ & |k_u| = 1 \\ & |k_y| = 1, \end{aligned} \tag{21}$$

where $P = R_0 + z R_1$ (18). Solving the optimization problem (21), optimal blending vectors and the corresponding minimum feedback gain (19) are obtained. Hence, the computation of the overall controller K is reduced to solving (21).

3.2 Efficient Blending Vector Computation

In this subsection, a numerically efficient algorithm for solving the blending vector design problem (21) is derived. The algorithm is described without loss of generality for a system with $n_u = 2$ inputs and $n_y = 2$ outputs. For systems with $n_u > 2$ or $n_y > 2$, a dynamic mode can always be expressed as

$$\begin{aligned} M(s) &= C(sI - A)^{-1} B \\ &= Q_C \underbrace{R_C (sI - A)^{-1} R_B^T}_{\tilde{M}(s)} Q_B^T, \end{aligned} \tag{22}$$

where both $Q_C \in \mathbb{R}^{n_y \times n_{\tilde{y}}}$ and $Q_B \in \mathbb{R}^{n_u \times n_{\tilde{u}}}$ form orthonormal bases and $\tilde{M}(s)$ is a transfer function ma-

trix with $n_{\tilde{u}} \leq 2$ inputs and $n_{\tilde{y}} \leq 2$ outputs (Pusch and Ossmann, 2019b). To that end, $B^T = Q_B R_B$ and $C = Q_C R_C$ from a minimal realization $\{A, B, C\}$ of $M(s)$ are decomposed using, e.g., a thin QR decomposition. Hence, the input and output blending vectors $\tilde{k}_u$ and $\tilde{k}_y$ for controlling $\tilde{M}(s)$ can be computed as follows and blending vectors for the original mode $M(s)$ are obtained as

$$k_u = Q_B \tilde{k}_u \quad \text{and} \quad k_y = Q_C \tilde{k}_y. \tag{23}$$

Note that thereby, Q_B and Q_C act as unitary transformations such that neither the objective function nor the length of the blending vectors is affected.

For efficiently computing the optimal blending vectors considering $n_u = 2$ inputs and $n_y = 2$ outputs, the pole placement constraint $k_y^T P k_u = 0$ from (18) is used to reduce the number of decision variables in (21). To that end, three different cases need to be distinguished depending on the rank of P, which is at most two as discussed above.

Case 1 ($\operatorname{rank} P = 2$). Since P has full rank, the constraint $k_y^T P k_u = 0$ can only be satisfied when k_y is orthogonal to Pk_u. This allows computing the output blending vector k_y from a given input blending vector k_u. Define the permutation matrix

$$\Pi = \begin{bmatrix} 0 & -1 \\ 1 & 0 \end{bmatrix}. \tag{24}$$

A suitable output blending vector then is

$$k_y = \pm \frac{\Pi P k_u}{|P k_u|}. \tag{25}$$

Note that in (25), the output blending vector is normalized to length one, i.e., the constraint $|k_y| = 1$ is achieved. To ensure the same for the input blending vector, k_u is expressed in polar coordinates as

$$k_u = \begin{bmatrix} \cos\phi \\ \sin\phi \end{bmatrix}. \tag{26}$$

As a result, $k_u(\phi)$ depends on the single parameter $\phi \in \mathbb{R}$. From (25), $k_y(k_u(\phi))$ is also uniquely determined through ϕ. Hence, the optimization problem (21) can be equivalently reformulated as the unconstrained optimization problem

$$\max_{\phi \in \mathbb{R}} \frac{|k_u(\phi)^T P^T \Pi^T R_1 k_u(\phi)|}{|P k_u(\phi)|}. \tag{27}$$

From $\phi^* \in \mathbb{R}$ solving (27), optimal input and output blending vectors are directly computed according to (26) and (25) as $k_u^* = [\cos\phi^* \ \ \sin\phi^*]^T$ and $k_y^* = \Pi P k_u^* / |P k_u^*|$, respectively.

Case 2 ($\operatorname{rank} P = 1$). If $\operatorname{rank} P = 1$, the matrix P can be decomposed as $P = q r^T$ with $q \in \mathbb{R}^2$ and $r \in \mathbb{R}^2$. Consequently, the pole placement constraint (18) can be reformulated as

$$k_y^T q r^T k_u = 0 \ \Leftrightarrow \ k_y^T q = 0 \ \vee \ r^T k_u = 0. \tag{28}$$

The two equality constraints on the right-hand side of (28) yield candidates for optimal input and output blending vectors. Using again the permutation matrix Π from (24), these candidate vectors can be expressed as

$$k_y^T q = 0 \ \Rightarrow \ k_{y,1}^* = \pm \Pi \frac{q}{|q|} \ \Rightarrow \ k_{u,1}^* = \frac{R_1^T k_{y,1}^*}{|R_1^T k_{y,1}^*|}, \tag{29}$$

$$r^T k_u = 0 \ \Rightarrow \ k_{u,2}^* = \pm \Pi \frac{r}{|r|} \ \Rightarrow \ k_{y,2}^* = \frac{R_1 k_{u,2}^*}{|R_1 k_{u,2}^*|}. \tag{30}$$

The idea behind (29) and (30) is to first satisfy the constraint $k_y^T P k_u = 0$ by finding a candidate vector $k_{y,1}^*$ or $k_{u,2}^*$ which is orthogonal to q or r, respectively. The objective function $|k_y^T R_1 k_u|$ from (21) is then maximized when the remaining candidate vector $k_{u,1}^*$ is parallel to $(k_{y,1}^*)^T R_1$ or $k_{y,2}^*$ is parallel to $R_1 k_{u,2}^*$. Thus, the optimal pair of blending vectors can be selected through direct search as the one which yields the maximum objective function $|(k_{y,i}^*)^T R_1 k_{u,i}^*|$ with $i = 1, 2$.

Case 3 ($\operatorname{rank} P = 0$). In case $\operatorname{rank} P = 0$, the constraint $k_y^T P k_u = 0$ vanishes and the optimal blending vectors k_y^* and k_u^* are directly obtained from a singular value decomposition (SVD) on R_1. More specifically, the objective $|k_y^T R_1 k_u|$ is maximized by choosing k_y and k_u as the left and right singular vectors associated with the largest singular value of R_1.

3.3 Special Cases

This subsection discusses special cases of the proposed pole placement method that either simplify the computation of the blending vectors or are of conceptual interest.

Active Damping. When the control objective is to increase relative damping of an individual mode without affecting its natural frequency, i.e., $\zeta_{\mathrm{cl}} > \zeta$ and $\omega_{\mathrm{n,cl}} = \omega_{\mathrm{n}}$, the poles are shifted along a circle around the origin, see Fig. 2. In that case, (14) states that $r_0 = 0$ for $\lambda \neq 0$. That is, the optimal blending of inputs and outputs places the zero of the blended mode's transfer function at $z = 0$, see (16). While this does not affect the algorithm described in Section 3.2, it establishes connections to other commonly encountered control techniques. As a zero at the origin is the frequency domain equivalent to differentiation, the blended measurement signal can be interpreted as a generalized velocity of the dynamic mode, cf. Hanel (2001); Danowsky et al. (2013); Theis et al. (2015, 2020). Feeding back such a velocity naturally increases modal damping (e.g. Balas, 1978; Preumont, 1997; Pusch and Ossmann, 2019a).

Shifting Poles Parallel to the Imaginary Axis. When the given open-loop poles and desired closed-loop poles have the same real part, i.e., $\Re(p) = \Re(p_{\mathrm{cl}})$, $\zeta\omega_{\mathrm{n}} = \zeta_{\mathrm{cl}}\omega_{\mathrm{n,cl}}$ and (16) becomes singular. It follows from (15) that $r_1 = 0$ for $\lambda \neq 0$. As a result, the new pole placement constraint is $k_y^T R_1 k_u = 0$ instead of (18). Further, the objective function (20) is replaced by $\max |k_y^T R_0 k_u|$, as $\min |\lambda|$ with $\lambda = (\omega_{\mathrm{n}}^2 - \omega_{\mathrm{n,cl}}^2)/r_0$ from (14) is now equivalent to $\max |r_0|$. Summing up, the blending vector design problem for the singular case $\zeta\omega_{\mathrm{n}} = \zeta_{\mathrm{cl}}\omega_{\mathrm{n,cl}}$ is given as

$$\begin{aligned} \underset{k_u \in \mathbb{R}^{n_u}, k_y \in \mathbb{R}^{n_y}}{\text{maximize}} \quad & |k_y^T R_0 k_u| \\ \text{subject to} \quad & k_y^T R_1 k_u = 0 \\ & |k_u| = 1 \\ & |k_y| = 1 \end{aligned} \tag{31}$$

and can be solved again as described in Section 3.2.

Real-valued Poles. In case the targeted mode features only a single real-valued pole $p \in \mathbb{R}$, i.e., the transfer function is $M(s) = c(s-p)^{-1}b^T$ with $b \in \mathbb{R}^{n_u}$ and $c \in \mathbb{R}^{n_y}$, the pole can only be shifted along the real axis. In that case, the open- and closed-loop transfer function of the blended mode are given as

$$m(s) = k_y^T M(s) k_u = \frac{k_y^T c b^T k_u}{s - p} \tag{32}$$

and

$$m_{\mathrm{cl}}(s) = \frac{m(s)}{1 - \lambda m(s)} = \frac{k_y^T c b k_u}{s - \underbrace{(p + \lambda k_y^T c b k_u)}_{p_{\mathrm{cl}}}}. \tag{33}$$

From (33), the feedback gain required to place the closed-loop pole at $p_{\mathrm{cl}} \in \mathbb{R}$ is directly given as

$$\lambda = \frac{p_{\mathrm{cl}} - p}{k_y^T c b k_u}. \tag{34}$$

Its absolute value is minimized when the blending vectors of unit length are chosen as

$$k_u^* = \frac{b}{|b|} \quad \text{and} \quad k_y^* = \frac{c}{|c|}. \tag{35}$$

In case it is desired to shift a conjugate complex pole pair onto the real axis, the resulting mode can be seen as an overdamped system with two poles $p_1 \in \mathbb{R}$ and $p_2 \in \mathbb{R}$ on the real axis. In that case, it follows from $(s - p_1)(s - p_2) = s^2 + 2\zeta\omega_{\mathrm{n}} + \omega_{\mathrm{n}}^2$ that

$$\omega_{\mathrm{n}}^2 = p_1 p_2 \quad \text{and} \quad 2\omega_{\mathrm{n}}\zeta = -p_1 - p_2. \tag{36}$$

Substituting (36) in (16), the same algorithm as described in Section 3.2 can again be used.

Single Input or Single Output Systems. For a system with a single input but $n_y > 1$ linearly independent outputs, it follows from (18) that $P \in \mathbb{R}^{n_y \times 1}$. In that case, the optimal blending vectors, which solve the optimization problem (21), are directly obtained from the constraint (18) as

$$k_u^* = 1 \quad \text{and} \quad k_y^* = \pm \Pi P / |P|, \tag{37}$$

where the permutation matrix Π is defined in (24). Similarly, for a system with a single output but $n_u > 1$ linearly independent inputs, $P \in \mathbb{R}^{1 \times n_u}$ and

$$k_u^* = \pm \Pi P^T / |P| \quad \text{and} \quad k_y^* = 1. \tag{38}$$

Note that this case of only a single input or a single output greatly simplifies the computation of the optimal blending vectors.

3.4 Mode Decoupling

So far, the proposed pole placement algorithm only considers a single targeted mode. However, the other modes of the system may still be excited by the blended inputs or measured by the blended outputs. This effect is commonly known as spillover. To avoid spillover, the targeted mode needs to be decoupled from all other modes. This can be achieved by applying dynamic filters such as band-stops to the measurements before designing the blending vectors. For this to work, the targeted and residual modes need to be well separated in frequency. If this is not the case, it is proposed to enforce orthogonality of the blending vectors and the mode shapes of residual modes. More specifically, orthogonality is enforced on the corresponding pole input and output vectors introduced in Section 2 .

The reasoning is that a residual mode $M_r(s)$ is uncontrollable from a blended control input when

$$k_u^T b_{p_r} = 0, \tag{39}$$

where $b_{p_r} \in \mathbb{C}^{n_u}$ denotes the pole input vector of the residual mode r. Similarly, M_r is unobservable from a blended measurement output when

$$k_y^T c_{p_r} = 0, \tag{40}$$

where $c_{p_r} \in \mathbb{C}^{n_y}$ denotes the pole output vector of the residual mode r. To enforce mode decoupling, both the real and imaginary parts of the pole input and output vectors of all considered residual modes are collected as column vectors in the matrices R_u and R_y, respectively. Note that R_u and R_y are real-valued and span the same subspaces as the complex input and output vectors and their complex conjugates. Eventually, the mode decoupling constraints are formulated as

$$k_u^T R_u = 0, \tag{41}$$

$$k_y^T R_y = 0. \tag{42}$$

These constraints are then added to the blending vector design problem derived in Section 3.1. Consequently, the blending vectors k_u and k_y are restricted to the null space of R_u^T and R_y^T, respectively. If one of the null spaces is empty, i.e., $\operatorname{rank} R_u = n_u$ or $\operatorname{rank} R_y = n_y$, the decoupled blending vector design problem is infeasible. This also implies that for a finite number of inputs and outputs, the number of residual modes which can be made uncontrollable or unobservable is limited. Note, however, that for mode decoupling it may be sufficient to make the residual modes either uncontrollable or unobservable but not both.

In order to solve the blending vector design problem augmented with the mode decoupling constraints (41) and (42), the original optimization variables k_u and k_y are replaced by

$$k_u = N_u \hat{k}_u \quad \text{and} \quad k_y = N_y \hat{k}_y, \tag{43}$$

where N_u and N_y denote orthonormal bases of the null spaces of R_u^T and R_y^T, respectively. The blended mode then becomes

$$k_y^T M(s) k_u = \hat{k}_y^T \underbrace{N_y^T M(s) N_u}_{\hat{M}(s)} \hat{k}_u, \tag{44}$$

which means that the decoupling constraints are incorporated into the design by simply replacing the original targeted mode $M(s)$ with $\hat{M}(s) = N_y^T M(s) N_u$. Solving the optimization problem (21) for $\hat{M}(s)$ instead of $M(s)$ yields the optimal blending vectors $\hat{k}_u^*$ and $\hat{k}_y^*$, from which the actual blending vectors $k_u^* = N_u \hat{k}_u^*$ and $k_y^* = N_u \hat{k}_u^*$ are then obtained according to (43). Since N_u and N_y act as unitary linear transformations, neither the objective function nor the norm of the blending vectors is changed.

Note that the null spaces for mode decoupling must be included before the decomposition (22) reduces the system to at most two inputs and outputs, see also the summary in Section 3.5. Note further that the additional mode decoupling constraints typically increase the required feedback gain λ. Hence, the designer must trade off the importance of decoupling from individual modes and the drawbacks associated with a larger feedback gain.

3.5 Summary of the Proposed Algorithm

In order to allow for a straightforward application of the proposed pole placement approach, the findings of Sections 3.1 to 3.4 are summarized as follows. The control objective is to shift the natural frequency and relative damping of an oscillating mode $M(s)$ from $\omega_\mathrm{n} \to \omega_\mathrm{n,cl}$ and from $\zeta \to \zeta_\mathrm{cl}$, respectively. To decouple $M(s)$ from other modes, the null spaces N_u and N_y are computed as described in Section 3.4. Then, a decomposition as stated in (22) yields

$$N_y^T M(s) N_u = Q_C \frac{R_1 s + R_0}{s^2 + 2\zeta\omega_\mathrm{n} s + \omega_\mathrm{n}^2} Q_B^T, \tag{45}$$

where R_0 and R_1 are real-valued matrices of maximum dimension 2×2, and both Q_B and Q_C form orthogonal bases. According to (26) and (25), the optimal blending vectors for the generic case $\zeta\omega_\mathrm{n} \neq \zeta_\mathrm{cl}\omega_\mathrm{n,cl}$ are

$$k_u(\phi) = \begin{bmatrix} \cos\phi \\ \sin\phi \end{bmatrix} \quad \text{and} \quad k_y(\phi) = \pm \frac{\Pi P k_u(\phi)}{|P k_u(\phi)|}, \tag{46}$$

where

$$\Pi = \begin{bmatrix} 0 & -1 \\ 1 & 0 \end{bmatrix} \quad \text{and} \quad P = R_0 + \underbrace{\frac{\omega_\mathrm{n,cl}^2 - \omega_\mathrm{n}^2}{2(\zeta\omega_\mathrm{n} - \zeta_\mathrm{cl}\omega_\mathrm{n,cl})}}_{z} R_1. \tag{47}$$

Solving the equivalent optimization problem (27) yields

$$\phi^* = \arg\max_\phi \frac{|k_u(\phi)^T P^T \Pi^T R_1 k_u(\phi)|}{|P k_u(\phi)|}, \tag{48}$$

which allows computation of $k_u(\phi^*)$ and $k_y(\phi^*)$ by inserting $\phi = \phi^*$ into (46). Combining (23) and (43), the optimal input and output blending vectors are then obtained as

$$k_u^* = N_u Q_B k_u(\phi^*) \quad \text{and} \quad k_y^* = N_y Q_C k_y(\phi^*). \tag{49}$$

Eventually, the desired closed-loop dynamics are achieved by closing the loop with the feedback controller

$$K = \lambda^* k_u^* k_y^{*T}, \tag{50}$$

where the feedback gain with minimum magnitude is computed according to (19) as

$$\lambda^* = 2 \frac{\zeta\omega_\mathrm{n} - \zeta_\mathrm{cl}\omega_\mathrm{n,cl}}{k_y(\phi^*)^T R_1 k_u(\phi^*)}. \tag{51}$$

Note that (46)–(48) assume the case $\operatorname{rank} P = 2$. The computation greatly simplifies in case $\operatorname{rank} P < 2$ or when only a single input or output is considered, see Sections 3.2 and 3.3. For the singular case with $\zeta\omega_\mathrm{n} = \zeta_\mathrm{cl}\omega_\mathrm{n,cl}$, the matrix R_1 is replaced by R_0 and P is replaced by R_1 in (46) and (48). The optimal blending vectors are then computed in the same way, but the feedback gain is $\lambda^* = \frac{\omega_\mathrm{n}^2 - \omega_\mathrm{n,cl}^2}{k_y(\phi^*)^T R_1 k_u(\phi^*)}$ as given in Section 3.3.

4. NUMERICAL EXAMPLE

To demonstrate the pole placement approach, the oscillating mode $M(s) = C\,(sI - A)^{-1} B$ with

$$A = \begin{bmatrix} -1 & 1 \\ -1 & -1 \end{bmatrix}, B = \begin{bmatrix} 0.78 & 1.20 \\ 1.17 & -0.79 \end{bmatrix}, C = \begin{bmatrix} 1.74 & 3.14 \\ -3.11 & 1.69 \end{bmatrix}$$

is considered, which features a natural frequency $\omega_\mathrm{n} = \sqrt{2}$ and a relative damping $\zeta = 1/\sqrt{2}$. The control objective is to achieve critical damping, i.e., $\zeta_\mathrm{cl} = 1$, while the natural frequency should remain unaffected, i.e., $\omega_\mathrm{n,cl} = \omega_\mathrm{n} = \sqrt{2}$. In other words, it is desired to move the open-loop conjugate complex pole pair $p_{1,2} = -1 \pm 1\mathrm{j}$ onto the real axis as $p_1 = p_2 = -1$ by closing the loop. Note that increasing the damping without changing the frequency of a conjugate complex pole pair is considered as *active damping* and discussed in detail in Section 3.3. The required zero location according to (16) is at $z = 0$, which results in $P = R_0$ when inserted into (18). Solving the unconstrained optimization problem (27) yields $\phi^* = 0.333$. Inserting this value to (25) and (26) yields the optimal input and output blending vectors

$$k_u^* = \begin{bmatrix} 0.326 \\ 0.945 \end{bmatrix} \quad \text{and} \quad k_y^* = \begin{bmatrix} -0.855 \\ 0.518 \end{bmatrix}.$$

From (19), the corresponding minimum feedback gain is $\lambda^* = -0.227$. Hence, the resulting feedback controller is

$$K = \lambda^* k_u^* k_y^{*T} = \begin{bmatrix} -0.031 & 0.067 \\ -0.091 & 0.195 \end{bmatrix}. \tag{52}$$

Note that the optimization problem (27) has multiple solutions as, in fact, $\phi^* = 0.333 + k\pi, k \in \mathbb{Z}$. This ambiguity affects the signs of k_u^* and k_y^*, but cancels out in multiplication. Therefore, the resulting controller K is uniquely given by (52).

To illustrate the principle further, the absolute feedback gain $|\lambda|$ required for placing the conjugate complex pole pair at other locations in the complex plane is computed and depicted in Fig. 3. As expected, $|\lambda|$ increases with the distance of the closed-loop pole from the open-loop pole. Additional solid lines in Fig. 3 summarize the possible closed-loop pole locations which require the same zero z. The dashed line indicates the singular case $\omega_\mathrm{n}\zeta = \omega_\mathrm{n,cl}\zeta_\mathrm{cl}$, which can be interpreted as $z = \infty$. For $z = 0$, the natural frequency remains constant and only the relative damping is affected. Note that Fig. 3 shows only the positive imaginary part due to symmetry with respect to the real axis.

REFERENCES

Balas, M. (1978). Feedback control of flexible systems. *IEEE Transactions on Automatic Control*, 673–679. doi: 10.1109/TAC.1978.1101798.

Danowsky, B., Kotikalpudi, A., Schmidt, D., Regan, C., and Seiler, P. (2018). Flight testing flutter suppression on a small flexible flying-wing aircraft. In *Multidisciplinary Analysis and Optimization Conf.* Atlanta, USA.

Danowsky, B., Thompson, P., Lee, D.C., and Brenner, M. (2013). Modal isolation and damping for adaptive aeroservoelastic suppression. In *AIAA Atmospheric Flight Mechanics Conference*. Boston, USA.

Franke, M. (2014). Eigenvalue assignment by static output feedback - on a new solvability condition and the com-

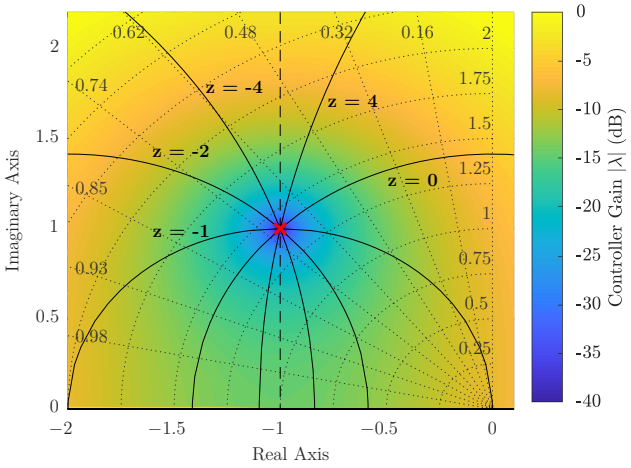

Fig. 3. Illustration of the feedback gain magnitude required for shifting the given pole (✕) in the complex plane. Constant values of the zero z introduced by blending inputs and outputs are marked as solid lines. The dashed vertical line indicates the singular case $z = \infty$.

putation of low gain feedback matrices. *International Journal of Control*, 87(1), 64–75.

Hanel, M. (2001). *Robust integrated flight and aeroelastic control system design for a large transport aircraft*. Ph.D. thesis, Dissertation, Universität Stuttgart.

Hoogendijk, R., Heertjesand, M., van de Molengraft, R., and Steinbuch, M. (2014). Directional notch filters for motion control of flexible structures. *Mechatronics*, 24(6), 632–639.

Kailath, T. (1980). *Linear systems*, volume 156. Prentice-Hall Englewood Cliffs, NJ.

Kimura, H. (1994). Pole assignment by output feedback: A longstanding open problem. In *Proceedings of the 33rd IEEE Conference on Decision and Control*. Lake Buena Vista, USA.

Kiritsis, K.H. (2002). A necessary condition for pole assignment by constant output feedback. *Systems & control letters*, 45(4), 317–320.

Preumont, A. (1997). *Vibration control of active structures*. Springer.

Pusch, M. (2018). Aeroelastic mode control using $\mathcal{H}_2$-optimal blends for inputs and outputs. In *AIAA Guidance, Navigation, & Control Conference*. Orlando, USA.

Pusch, M. and Ossmann, D. (2019a). Blending of inputs and outputs for modal velocity feedback. In *27th IEEE Mediterranean Conference on Control and Automation*. Akko, Israel.

Pusch, M. and Ossmann, D. (2019b). $\mathcal{H}_2$-optimal Blending of Inputs and Outputs for Modal Control. *IEEE Transaction of Control System Technology*.

Pusch, M., Ossmann, D., Dillinger, J., Kier, T.M., Tang, M., and Lübker, J. (2019). Aeroelastic modeling and control of an experimental flexible wing. In *AIAA Guidance, Navigation, & Control Conference*. San Diego, USA.

Rosenthal, J. and Willems, J. (1999). Open problems in the area of pole placement. In *Open problems in mathematical systems and control theory*, 181–191. Springer.

Syrmos, V., Abdallah, C., Dorato, P., and Grigoriadis, K. (1997). Static output feedback - a survey. *Automatica*, 33(2), 125–137.

Theis, J., Pfifer, H., Balas, G., and Werner, H. (2015). Integrated flight control design for a large flexible aircraft. In *American Control Conference (ACC)*, 3830–3835. Chicago, USA. doi:10.1109/ACC.2015.7171927.

Theis, J., Pfifer, H., and Seiler, P. (2020). Robust modal damping control for active flutter suppression. doi:10.2514/1.G004846. J. Guid., Control, Dyn.

Wang, X. (1992). Pole placement by static output feedback. *Journal of Math. Systems, Estimation, and Control*, 2, 205–218.

Willems, J. and Hesselink, W. (1978). Generic properties of the pole placement problem. *IFAC Proceedings Volumes*, 11(1), 1725–1729.

Yang, K. and Orsi, R. (2007). Static output feedback pole placement via a trust region approach. *IEEE Transactions on Automatic Control*, 52(11), 2146–2150.